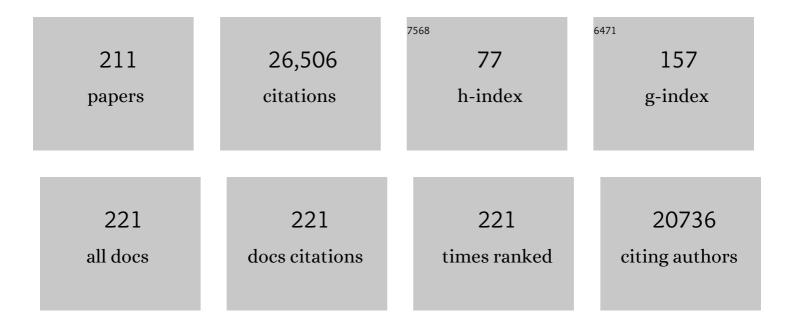
## **Steve Weiner**

List of Publications by Year in descending order

Source: https://exaly.com/author-pdf/1730114/publications.pdf Version: 2024-02-01



#	Article	IF	CITATIONS
1	Persistence of soil organic matter as an ecosystem property. Nature, 2011, 478, 49-56.	27.8	4,243
2	Taking Advantage of Disorder: Amorphous Calcium Carbonate and Its Roles in Biomineralization. Advanced Materials, 2003, 15, 959-970.	21.0	1,344
3	Mollusk Shell Formation: A Source of New Concepts for Understanding Biomineralization Processes. Chemistry - A European Journal, 2006, 12, 980-987.	3.3	919
4	Sea Urchin Spine Calcite Forms via a Transient Amorphous Calcium Carbonate Phase. Science, 2004, 306, 1161-1164.	12.6	881
5	Calcitic microlenses as part of the photoreceptor system in brittlestars. Nature, 2001, 412, 819-822.	27.8	605
6	Mollusc larval shell formation: amorphous calcium carbonate is a precursor phase for aragonite. The Journal of Experimental Zoology, 2002, 293, 478-491.	1.4	572
7	Bone hierarchical structure in three dimensions. Acta Biomaterialia, 2014, 10, 3815-3826.	8.3	501
8	Amorphous calcium phosphate is a major component of the forming fin bones of zebrafish: Indications for an amorphous precursor phase. Proceedings of the National Academy of Sciences of the United States of America, 2008, 105, 12748-12753.	7.1	490
9	Structure of the Nacreous Organic Matrix of a Bivalve Mollusk Shell Examined in the Hydrated State Using Cryo-TEM. Journal of Structural Biology, 2001, 135, 8-17.	2.8	476
10	Factors Involved in the Formation of Amorphous and Crystalline Calcium Carbonate:Â A Study of an Ascidian Skeleton. Journal of the American Chemical Society, 2002, 124, 32-39.	13.7	458
11	Crystallization Pathways in Biomineralization. Annual Review of Materials Research, 2011, 41, 21-40.	9.3	456
12	Mapping amorphous calcium phosphate transformation into crystalline mineral from the cell to the bone in zebrafish fin rays. Proceedings of the National Academy of Sciences of the United States of America, 2010, 107, 6316-6321.	7.1	389
13	Transformation mechanism of amorphous calcium carbonate into calcite in the sea urchin larval spicule. Proceedings of the National Academy of Sciences of the United States of America, 2008, 105, 17362-17366.	7.1	380
14	Mineralogical and compositional changes in bones exposed on soil surfaces in Amboseli National Park, Kenya: diagenetic mechanisms and the role of sediment pore fluids. Journal of Archaeological Science, 2004, 31, 721-739.	2.4	342
15	STRUCTURAL BIOLOGY: Choosing the Crystallization Path Less Traveled. Science, 2005, 309, 1027-1028.	12.6	322
16	Diagenesis in Prehistoric Caves: the Use of Minerals that Form In Situ to Assess the Completeness of the Archaeological Record. Journal of Archaeological Science, 2000, 27, 915-929.	2.4	300
17	Mollusk shell formation: Mapping the distribution of organic matrix components underlying a single aragonitic tablet in nacre. Journal of Structural Biology, 2006, 153, 176-187.	2.8	296
18	Sediments exposed to high temperatures: reconstructing pyrotechnological processes in Late Bronze and Iron Age Strata at Tel Dor (Israel). Journal of Archaeological Science, 2007, 34, 358-373.	2.4	241

#	Article	IF	CITATIONS
19	Ash Deposits in Hayonim and Kebara Caves, Israel: Macroscopic, Microscopic and Mineralogical Observations, and their Archaeological Implications. Journal of Archaeological Science, 1996, 23, 763-781.	2.4	233
20	Control Over Aragonite Crystal Nucleation and Growth: An In Vitro Study of Biomineralization. Chemistry - A European Journal, 1998, 4, 389-396.	3.3	229
21	Bone mineralization proceeds through intracellular calcium phosphate loaded vesicles: A cryo-electron microscopy study. Journal of Structural Biology, 2011, 174, 527-535.	2.8	227
22	Mollusk Shell Acidic Proteins: In Search of Individual Functions. ChemBioChem, 2003, 4, 522-529.	2.6	220
23	Asprich: A Novel Aspartic Acid-Rich Protein Family from the Prismatic Shell Matrix of the Bivalve Atrina rigida. ChemBioChem, 2005, 6, 304-314.	2.6	220
24	Structural Characterization of the Transient Amorphous Calcium Carbonate Precursor Phase in Sea Urchin Embryos. Advanced Functional Materials, 2006, 16, 1289-1298.	14.9	219
25	Spiers Memorial Lecture : Lessons from biomineralization: comparing the growth strategies of mollusc shell prismatic and nacreous layers in Atrina rigida. Faraday Discussions, 2007, 136, 9.	3.2	217
26	Stability of phytoliths in the archaeological record: a dissolution study of modern and fossil phytoliths. Journal of Archaeological Science, 2011, 38, 2480-2490.	2.4	216
27	Black-Coloured Bones in Hayonim Cave, Israel: Differentiating Between Burning and Oxide Staining. Journal of Archaeological Science, 1997, 24, 439-446.	2.4	213
28	Polysaccharides of Intracrystalline Glycoproteins Modulate Calcite Crystal Growth In Vitro. Chemistry - A European Journal, 1996, 2, 278-284.	3.3	209
29	Bat guano and preservation of archaeological remains in cave sites. Journal of Archaeological Science, 2004, 31, 1259-1272.	2.4	209
30	Role of Magnesium Ion in the Stabilization of Biogenic Amorphous Calcium Carbonate: A Structureâ <sup>~</sup> Function Investigation. Chemistry of Materials, 2010, 22, 161-166.	6.7	204
31	Modern and fossil charcoal: aspects of structure and diagenesis. Journal of Archaeological Science, 2006, 33, 428-439.	2.4	202
32	Mode of Occupation of Tabun Cave, Mt Carmel, Israel During the Mousterian Period: A Study of the Sediments and Phytoliths. Journal of Archaeological Science, 1999, 26, 1249-1260.	2.4	199
33	Geo-Ethnoarchaeology of Pastoral Sites: The Identification of Livestock Enclosures in Abandoned Maasai Settlements. Journal of Archaeological Science, 2003, 30, 439-459.	2.4	193
34	Three-dimensional structure of human lamellar bone: The presence of two different materials and new insights into the hierarchical organization. Bone, 2014, 59, 93-104.	2.9	193
35	Biologically Formed Amorphous Calcium Carbonate. Connective Tissue Research, 2003, 44, 214-218.	2.3	187
36	Distinguishing between calcites formed by different mechanisms using infrared spectrometry: archaeological applications. Journal of Archaeological Science, 2010, 37, 3022-3029.	2.4	182

#	Article	IF	CITATIONS
37	Phytolith-rich layers from the Late Bronze and Iron Ages at Tel Dor (Israel): mode of formation and archaeological significance. Journal of Archaeological Science, 2008, 35, 57-75.	2.4	179
38	The phytolith archaeological record: strengths and weaknesses evaluated based on a quantitative modern reference collection from Greece. Journal of Archaeological Science, 2007, 34, 1262-1275.	2.4	170
39	The grinding tip of the sea urchin tooth exhibits exquisite control over calcite crystal orientation and Mg distribution. Proceedings of the National Academy of Sciences of the United States of America, 2009, 106, 6048-6053.	7.1	161
40	Geoarchaeology in an urban context: The uses of space in a Phoenician monumental building at Tel Dor (Israel). Journal of Archaeological Science, 2005, 32, 1417-1431.	2.4	158
41	Three-dimensional Distribution of Minerals in the Sediments of Hayonim Cave, Israel: Diagenetic Processes and Archaeological Implications. Journal of Archaeological Science, 2002, 29, 1289-1308.	2.4	156
42	Radiocarbon dating of charcoal and bone collagen associated with early pottery at Yuchanyan Cave, Hunan Province, China. Proceedings of the National Academy of Sciences of the United States of America, 2009, 106, 9595-9600.	7.1	153
43	A hydrated crystalline calcium carbonate phase: Calcium carbonate hemihydrate. Science, 2019, 363, 396-400.	12.6	153
44	The Mechanism of Color Change in the Neon Tetra Fish: a Lightâ€Induced Tunable Photonic Crystal Array. Angewandte Chemie - International Edition, 2015, 54, 12426-12430.	13.8	152
45	Relatively well preserved DNA is present in the crystal aggregates of fossil bones. Proceedings of the National Academy of Sciences of the United States of America, 2005, 102, 13783-13788.	7.1	146
46	Materials design in biology. Materials Science and Engineering C, 2000, 11, 1-8.	7.3	145
47	Initial stages of calcium uptake and mineral deposition in sea urchin embryos. Proceedings of the National Academy of Sciences of the United States of America, 2014, 111, 39-44.	7.1	142
48	Phytoliths in the Middle Palaeolithic Deposits of Kebara Cave, Mt Carmel, Israel: Study of the Plant Materials used for Fuel and Other Purposes. Journal of Archaeological Science, 2000, 27, 931-947.	2.4	141
49	Ash Bones and Guano: a Study of the Minerals and Phytoliths in the Sediments of Grotte XVI, Dordogne, France. Journal of Archaeological Science, 2002, 29, 721-732.	2.4	141
50	Crystals, asymmetry and life. Nature, 2001, 411, 753-755.	27.8	140
51	Guanineâ€Based Biogenic Photonicâ€Crystal Arrays in Fish and Spiders. Advanced Functional Materials, 2010, 20, 320-329.	14.9	136
52	Transient precursor strategy in mineral formation of bone. Bone, 2006, 39, 431-433.	2.9	135
53	Structure and mechanical properties of the soft zone separating bulk dentin and enamel in crowns of human teeth: Insight into tooth function. Journal of Structural Biology, 2006, 153, 188-199.	2.8	134
54	Particle Accretion Mechanism Underlies Biological Crystal Growth from an Amorphous Precursor Phase. Advanced Functional Materials, 2014, 24, 5420-5426.	14.9	132

#	Article	IF	CITATIONS
55	Three-dimensional imaging of collagen fibril organization in rat circumferential lamellar bone using a dual beam electron microscope reveals ordered and disordered sub-lamellar structures. Bone, 2013, 52, 676-683.	2.9	131
56	Calcium Oxalate Crystals in Tomato and Tobacco Plants: Morphology and in Vitro Interactions of Crystal-Associated Macromolecules. Chemistry - A European Journal, 2001, 7, 1881-1888.	3.3	128
57	Stable Amorphous Calcium Carbonate Is the Main Component of the Calcium Storage Structures of the Crustacean Orchestia cavimana. Biological Bulletin, 2002, 203, 269-274.	1.8	126
58	Light Manipulation by Guanine Crystals in Organisms: Biogenic Scatterers, Mirrors, Multilayer Reflectors and Photonic Crystals. Advanced Functional Materials, 2017, 27, 1603514.	14.9	125
59	Reconstruction of spatial organization in abandoned Maasai settlements: implications for site structure in the Pastoral Neolithic of East Africa. Journal of Archaeological Science, 2004, 31, 1395-1411.	2.4	118
60	Biogenic Guanine Crystals from the Skin of Fish May Be Designed to Enhance Light Reflectance. Crystal Growth and Design, 2008, 8, 507-511.	3.0	118
61	Quality Controlled Radiocarbon Dating of Bones and Charcoal from the Early Pre-Pottery Neolithic B (PPNB) of Motza (Israel). Radiocarbon, 2005, 47, 193-206.	1.8	115
62	Forming nacreous layer of the shells of the bivalves Atrina rigida and Pinctada margaritifera: An environmental- and cryo-scanning electron microscopy study. Journal of Structural Biology, 2008, 162, 290-300.	2.8	115
63	An organic hydrogel as a matrix for the growth of calcite crystalsElectronic supplementary information (ESI) available: Scanning electron micrographs of calcite etched with EDTA. See http://www.rsc.org/suppdata/ob/b3/b309731e/. Organic and Biomolecular Chemistry, 2004, 2, 137.	2.8	113
64	Sea Urchin Tooth Design: An "Allâ€Calcite―Polycrystalline Reinforced Fiber Composite for Grinding Rocks. Advanced Materials, 2008, 20, 1555-1559.	21.0	111
65	Asprich mollusk shell protein: in vitro experiments aimed at elucidating function in CaCO3 crystallization. CrystEngComm, 2007, 9, 1171.	2.6	105
66	Mineral Assemblages in Theopetra, Greece: A Framework for Understanding Diagenesis in a Prehistoric Cave. Journal of Archaeological Science, 1999, 26, 1171-1180.	2.4	103
67	Quantitative Phytolith Study of Hearths from the Natufian and Middle Palaeolithic Levels of Hayonim Cave (Galilee, Israel). Journal of Archaeological Science, 2003, 30, 461-480.	2.4	97
68	Overview of the amorphous precursor phase strategy in biomineralization. Frontiers of Materials Science in China, 2009, 3, 104-108.	0.5	97
69	Differentiating between anthropogenic calcite in plaster, ash and natural calcite using infrared spectroscopy: implications in archaeology. Journal of Archaeological Science, 2008, 35, 905-911.	2.4	96
70	Human Root Dentin: Structural Anisotropy and Vickers Microhardness Isotropy. Connective Tissue Research, 1998, 39, 269-279.	2.3	95
71	Biomineralization: mineral formation by organisms. Physica Scripta, 2014, 89, 098003.	2.5	95
72	Decoupling Local Disorder and Optical Effects in Infrared Spectra: Differentiating Between Calcites with Different Origins. Advanced Materials, 2011, 23, 550-554.	21.0	91

#	Article	IF	CITATIONS
73	The image-forming mirror in the eye of the scallop. Science, 2017, 358, 1172-1175.	12.6	90
74	Structural Basis for the Brilliant Colors of the Sapphirinid Copepods. Journal of the American Chemical Society, 2015, 137, 8408-8411.	13.7	89
75	Calcite Crystal Growth by a Solidâ€6tate Transformation of Stabilized Amorphous Calcium Carbonate Nanospheres in a Hydrogel. Angewandte Chemie - International Edition, 2013, 52, 4867-4870.	13.8	88
76	Ethnoarchaeological study of phytolith assemblages from an agro-pastoral village in Northern Greece (Sarakini): development and application of a Phytolith Difference Index. Journal of Archaeological Science, 2008, 35, 600-613.	2.4	83
77	A perspective on underlying crystal growth mechanisms in biomineralization: solution mediated growth versus nanosphere particle accretion. CrystEngComm, 2015, 17, 2606-2615.	2.6	82
78	X-Ray absorption spectroscopy studies on the structure of a biogenic "amorphous―calcium carbonate phase â€. Dalton Transactions RSC, 2000, , 3977-3982.	2.3	81
79	Calcium Oxalate Stone Formation in the Inner Ear as a Result of an Slc26a4 Mutation. Journal of Biological Chemistry, 2010, 285, 21724-21735.	3.4	81
80	Opposite Particle Size Effect on Amorphous Calcium Carbonate Crystallization in Water and during Heating in Air. Chemistry of Materials, 2015, 27, 4237-4246.	6.7	80
81	Local Atomic Order and Infrared Spectra of Biogenic Calcite. Angewandte Chemie - International Edition, 2007, 46, 291-294.	13.8	76
82	Phosphate–Water Interplay Tunes Amorphous Calcium Carbonate Metastability: Spontaneous Phase Separation and Crystallization vs Stabilization Viewed by Solid State NMR. Journal of the American Chemical Society, 2015, 137, 990-998.	13.7	76
83	Certain Biominerals in Leaves Function as Light Scatterers. Advanced Materials, 2012, 24, OP77-83.	21.0	74
84	On the pathway of mineral deposition in larval zebrafish caudal fin bone. Bone, 2015, 75, 192-200.	2.9	74
85	Calcium transport into the cells of the sea urchin larva in relation to spicule formation. Proceedings of the National Academy of Sciences of the United States of America, 2016, 113, 12637-12642.	7.1	74
86	Tooth–PDL–bone complex: Response to compressive loads encountered during mastication – A review. Archives of Oral Biology, 2012, 57, 1575-1584.	1.8	73
87	The Stabilizing Effect of Silicate on Biogenic and Synthetic Amorphous Calcium Carbonate. Journal of the American Chemical Society, 2010, 132, 13208-13211.	13.7	71
88	Cryo-FIB-SEM serial milling and block face imaging: Large volume structural analysis of biological tissues preserved close to their native state. Journal of Structural Biology, 2016, 196, 487-495.	2.8	71
89	Detection of Burning of Plant Materials in the Archaeological Record by Changes in the Refractive Indices of Siliceous Phytoliths. Journal of Archaeological Science, 2003, 30, 217-226.	2.4	70
90	Iron and bronze production in Iron Age IIA Philistia: new evidence from Tell es-Safi/Gath, Israel. Journal of Archaeological Science, 2012, 39, 255-267.	2.4	68

#	Article	IF	CITATIONS
91	Remodeling in bone without osteocytes: Billfish challenge bone structure–function paradigms. Proceedings of the National Academy of Sciences of the United States of America, 2014, 111, 16047-16052.	7.1	68
92	Are tensile and compressive Young's moduli of compact bone different?. Journal of the Mechanical Behavior of Biomedical Materials, 2009, 2, 51-60.	3.1	65
93	Bone mineralization pathways during the rapid growth of embryonic chicken long bones. Journal of Structural Biology, 2016, 195, 82-92.	2.8	64
94	The 3D structure of the collagen fibril network in human trabecular bone: Relation to trabecular organization. Bone, 2015, 71, 189-195.	2.9	63
95	The Use of Raman Spectroscopy to Monitor the Removal of Humic Substances from Charcoal: Quality Control for <sup>14</sup> C Dating of Charcoal. Radiocarbon, 2002, 44, 1-11.	1.8	62
96	Mapping of tooth deformation caused by moisture change using moiré interferometry. Dental Materials, 2003, 19, 159-166.	3.5	62
97	Mineral Formation in the Larval Zebrafish Tail Bone Occurs via an Acidic Disordered Calcium Phosphate Phase. Journal of the American Chemical Society, 2016, 138, 14481-14487.	13.7	62
98	Nanosized particles in bone and dissolution insensitivity of bone mineral. Biointerphases, 2006, 1, 106-111.	1.6	61
99	The Structural Basis for Enhanced Silver Reflectance in Koi Fish Scale and Skin. Journal of the American Chemical Society, 2014, 136, 17236-17242.	13.7	61
100	Biomineralization of limpet teeth: A cryo-TEM study of the organic matrix and the onset of mineral deposition. Journal of Structural Biology, 2007, 158, 428-444.	2.8	60
101	Guanineâ€Based Photonic Crystals in Fish Scales Form from an Amorphous Precursor. Angewandte Chemie - International Edition, 2013, 52, 388-391.	13.8	60
102	Oxygen Spectroscopy and Polarization-Dependent Imaging Contrast (PIC)-Mapping of Calcium Carbonate Minerals and Biominerals. Journal of Physical Chemistry B, 2014, 118, 8449-8457.	2.6	60
103	BIOMINERALIZATION: At the Cutting Edge. Science, 2002, 298, 375-376.	12.6	57
104	Use of space in a Neolithic village in Greece (Makri): phytolith analysis and comparison of phytolith assemblages from an ethnographic setting in the same area. Journal of Archaeological Science, 2009, 36, 2342-2352.	2.4	56
105	Anisotropic mechanical properties of lamellar bone using miniature cantilever bending specimens. Journal of Biomechanics, 1999, 32, 647-654.	2.1	54
106	Guanine Crystallization in Aqueous Solutions Enables Control over Crystal Size and Polymorphism. Crystal Growth and Design, 2016, 16, 4975-4980.	3.0	54
107	The 9th century BCE destruction layer at Tell es-Safi/Gath, Israel: integrating macro- and microarchaeology. Journal of Archaeological Science, 2011, 38, 3471-3482.	2.4	53
108	New methods to isolate organic materials from silicified phytoliths reveal fragmented glycoproteins but no DNA. Quaternary International, 2009, 193, 11-19.	1.5	52

#	Article	IF	CITATIONS
109	Crystallization Pathways in Bone. Cells Tissues Organs, 2011, 194, 92-97.	2.3	52
110	Human impact around settlement sites: a phytolith and mineralogical study for assessing site boundaries, phytolith preservation, and implications for spatial reconstructions using plant remains. Journal of Archaeological Science, 2012, 39, 2697-2705.	2.4	51
111	Plant Cystoliths: A Complex Functional Biocomposite of Four Distinct Silica and Amorphous Calcium Carbonate Phases. Chemistry - A European Journal, 2012, 18, 10262-10270.	3.3	49
112	Biogenic Fish-gut Calcium Carbonate is a Stable Amorphous Phase in the Gilt-head Seabream, Sparus aurata. Scientific Reports, 2013, 3, 1700.	3.3	48
113	Lightâ€Induced Color Change in the Sapphirinid Copepods: Tunable Photonic Crystals. Advanced Functional Materials, 2016, 26, 1393-1399.	14.9	48
114	Ancient olive DNA in pits: preservation, amplification and sequence analysis. Journal of Archaeological Science, 2006, 33, 77-88.	2.4	46
115	Mineral-bearing vesicle transport in sea urchin embryos. Journal of Structural Biology, 2015, 192, 358-365.	2.8	46
116	Ion Pathways in Biomineralization: Perspectives on Uptake, Transport, and Deposition of Calcium, Carbonate, and Phosphate. Journal of the American Chemical Society, 2021, 143, 21100-21112.	13.7	44
117	Flint procurement strategies in the Late Lower Palaeolithic recorded by in situ produced cosmogenic 10Be in Tabun and Qesem Caves (Israel). Journal of Archaeological Science, 2005, 32, 207-213.	2.4	42
118	Geoarchaeological Investigation in a Domestic Iron Age Quarter, Tel Megiddo, Israel. Bulletin of the American Schools of Oriental Research, 2015, 374, 135-157.	0.2	42
119	Inter-trabecular angle: A parameter of trabecular bone architecture in the human proximal femur that reveals underlying topological motifs. Acta Biomaterialia, 2016, 44, 65-72.	8.3	41
120	Variations in Atomic Disorder in Biogenic Carbonate Hydroxyapatite Using the Infrared Spectrum Grinding Curve Method. Advanced Functional Materials, 2011, 21, 3308-3313.	14.9	40
121	Iron Age hydraulic plaster from Tell es-Safi/Gath, Israel. Journal of Archaeological Science, 2010, 37, 3000-3009.	2.4	39
122	Absolute Dating of the Late Bronze to Iron Age Transition and the Appearance of Philistine Culture in Qubur el-Walaydah, Southern Levant. Radiocarbon, 2015, 57, 77-97.	1.8	39
123	Optically functional isoxanthopterin crystals in the mirrored eyes of decapod crustaceans. Proceedings of the National Academy of Sciences of the United States of America, 2018, 115, 2299-2304.	7.1	39
124	The Organic Crystalline Materials of Vision: Structure–Function Considerations from the Nanometer to the Millimeter Scale. Advanced Materials, 2018, 30, e1800006.	21.0	38
125	Structural Characterization of Modern and Fossilized Charcoal Produced in Natural Fires as Determined by Using Electron Energy Loss Spectroscopy. Chemistry - A European Journal, 2007, 13, 2306-2310.	3.3	37
126	Tooth movements are guided by specific contact areas between the tooth root and the jaw bone: A dynamic 3D microCT study of the rat molar. Journal of Structural Biology, 2012, 177, 477-483.	2.8	37

#	Article	IF	CITATIONS
127	Plaster Characterization at the PPNB Site of Yiftahel (Israel) Including the Use of 14C: Implications for Plaster Production, Preservation, and Dating. Radiocarbon, 2012, 54, 887-896.	1.8	37
128	Tooth periodontal ligament: Direct 3D microCT visualization of the collagen network and how the network changes when the tooth is loaded. Journal of Structural Biology, 2013, 181, 108-115.	2.8	37
129	Cellular pathways of calcium transport and concentration toward mineral formation in sea urchin larvae. Proceedings of the National Academy of Sciences of the United States of America, 2020, 117, 30957-30965.	7.1	37
130	Biologically Controlled Morphology and Twinning in Guanine Crystals. Angewandte Chemie - International Edition, 2017, 56, 9420-9424.	13.8	36
131	Morphology of Goethite Crystals in Developing Limpet Teeth:  Assessing Biological Control over Mineral Formationâ€. Crystal Growth and Design, 2005, 5, 2131-2138.	3.0	35
132	Mineral and Matrix Components of the Operculum and Shell of the Barnacle <i>Balanus amphitrite</i> : Calcite Crystal Growth in a Hydrogel. Crystal Growth and Design, 2011, 11, 5122-5130.	3.0	35
133	Biomineralization pathways in a foraminifer revealed using a novel correlative cryo-fluorescence–SEM–EDS technique. Journal of Structural Biology, 2016, 196, 155-163.	2.8	34
134	Mineral Deposits in <i>Ficus</i> Leaves: Morphologies and Locations in Relation to Function. Plant Physiology, 2018, 176, 1751-1763.	4.8	34
135	Oxygen isotopic composition of opaline phytoliths: Potential for terrestrial climatic reconstruction. Geochimica Et Cosmochimica Acta, 1996, 60, 3949-3953.	3.9	33
136	Formation of Aragonite Crystals in the Crossed Lamellar Microstructure of Limpet Shells. Crystal Growth and Design, 2011, 11, 4850-4859.	3.0	33
137	Plants and Light Manipulation: The Integrated Mineral System in Okra Leaves. Advanced Science, 2017, 4, 1600416.	11.2	33
138	Aragonite Formation in the Chiton (Mollusca) Girdle. Helvetica Chimica Acta, 2003, 86, 1101-1112.	1.6	32
139	Anhydrous β-guanine crystals in a marine dinoflagellate: Structure and suggested function. Journal of Structural Biology, 2019, 207, 12-20.	2.8	32
140	Intercellular pathways from the vasculature to the forming bone in the zebrafish larval caudal fin: Possible role in bone formation. Journal of Structural Biology, 2019, 206, 139-148.	2.8	30
141	Three-dimensional structure of minipig fibrolamellar bone: Adaptation to axial loading. Journal of Structural Biology, 2014, 186, 253-264.	2.8	29
142	Mineralized biological materials: A perspective on interfaces and interphases designed over millions of years. Biointerphases, 2006, 1, P12-P14.	1.6	28
143	Control of Biogenic Nanocrystal Formation in Biomineralization. Israel Journal of Chemistry, 2016, 56, 227-241.	2.3	28
144	Radiocarbon Dating Shows an Early Appearance of Philistine Material Culture in Tell es-Safi/Gath, Philistia. Radiocarbon, 2015, 57, 825-850.	1.8	27

#	Article	IF	CITATIONS
145	The three-dimensional structure of anosteocytic lamellated bone of fish. Acta Biomaterialia, 2015, 13, 311-323.	8.3	27
146	Biomineralization pathways in calcifying dinoflagellates: Uptake, storage in MgCaP-rich bodies and formation of the shell. Acta Biomaterialia, 2020, 102, 427-439.	8.3	27
147	An integrated approach to reconstructing primary activities from pit deposits: iron smithing and other activities at Tel Dor under Neo-Assyrian domination. Journal of Archaeological Science, 2008, 35, 2895-2908.	2.4	26
148	Heating of flint debitage from Upper Palaeolithic contexts at Manot Cave, Israel: changes in atomic organization due to heating using infrared spectroscopy. Journal of Archaeological Science, 2015, 54, 45-53.	2.4	26
149	Characterization of unusual MgCa particles involved in the formation of foraminifera shells using a novel quantitative cryo SEM/EDS protocol. Acta Biomaterialia, 2018, 77, 342-351.	8.3	26
150	A highly reflective biogenic photonic material from core–shell birefringent nanoparticles. Nature Nanotechnology, 2020, 15, 138-144.	31.5	26
151	Design Strategy of Minipig Molars Using Electronic Speckle Pattern Interferometry: Comparison of Deformation under Load between the Toothâ€Mandible Complex and the Isolated Tooth. Advanced Materials, 2009, 21, 413-418.	21.0	25
152	Biologically Controlled Morphology and Twinning in Guanine Crystals. Angewandte Chemie, 2017, 129, 9548-9552.	2.0	25
153	Mineralization pathways in the active murine epiphyseal growth plate. Bone, 2020, 130, 115086.	2.9	25
154	Iron Age beehives at Tel Reá,¥ov in the Jordan valley. Antiquity, 2008, 82, 629-639.	1.0	24
155	Radiocarbon Concentrations of Wood Ash Calcite: Potential for Dating. Radiocarbon, 2011, 53, 117-127.	1.8	24
156	Biologically Formed Amorphous Calcium Carbonate. Connective Tissue Research, 2003, 44, 214-218.	2.3	24
157	Biologically formed amorphous calcium carbonate. Connective Tissue Research, 2003, 44 Suppl 1, 214-8.	2.3	24
158	The contents of unusual cone-shaped vessels (cornets) from the Chalcolithic of the southern Levant. Journal of Archaeological Science, 2009, 36, 629-636.	2.4	23
159	Bioâ€Inspired Materials – Mining the Old Literature for New Ideas. Advanced Materials, 2010, 22, 4547-4550.	21.0	23
160	Atomic order of aragonite crystals formed by mollusks. CrystEngComm, 2011, 13, 6780.	2.6	23
161	Achiral Calcium-Oxalate Crystals with Chiral Morphology from the Leaves of Some Solanacea Plants. Helvetica Chimica Acta, 2003, 86, 4007-4017.	1.6	21
162	Insights into whole bone and tooth function using optical metrology. Journal of Materials Science, 2007, 42, 8919-8933.	3.7	21

#	Article	IF	CITATIONS
163	The response of anosteocytic bone to controlled loading. Journal of Experimental Biology, 2015, 218, 3559-3569.	1.7	21
164	Direct MicroCT imaging of non-mineralized connective tissues at high resolution. Connective Tissue Research, 2014, 55, 52-60.	2.3	20
165	Alkane composition variations between darker and lighter colored comb beeswax. Apidologie, 2007, 38, 453-461.	2.0	19
166	Zebrafish skeleton development: High resolution micro-CT and FIB-SEM block surface serial imaging for phenotype identification. PLoS ONE, 2017, 12, e0177731.	2.5	18
167	Guanine and 7,8-Dihydroxanthopterin Reflecting Crystals in the Zander Fish Eye: Crystal Locations, Compositions, and Structures. Journal of the American Chemical Society, 2019, 141, 19736-19745.	13.7	18
168	Focused ion beam-SEM 3D analysis of mineralized osteonal bone: lamellae and cement sheath structures. Acta Biomaterialia, 2021, 121, 497-513.	8.3	18
169	The Contribution of Trabecular Bone to the Stiffness and Strength of Rat Lumbar Vertebrae. Spine, 2010, 35, E1153-E1159.	2.0	17
170	Microscale distribution and concentration of preserved organic molecules with carbon–carbon double bonds in archaeological ceramics: relevance to the field of residue analysis. Journal of Archaeological Science, 2014, 42, 509-518.	2.4	17
171	Preface—The Iron Age in Israel: The Exact and Life Sciences Perspectives. Radiocarbon, 2015, 57, 197-206.	1.8	17
172	A new method for extracting the insoluble occluded carbon in archaeological and modern phytoliths: Detection of 14C depleted carbon fraction and implications for radiocarbon dating. Journal of Archaeological Science, 2017, 78, 57-65.	2.4	17
173	Importance of the integrity of trabecular bone to the relationship between load and deformation of rat femora: an optical metrology study. Journal of Materials Chemistry, 2008, 18, 3855.	6.7	16
174	The Mechanism of Color Change in the Neon Tetra Fish: a Lightâ€Induced Tunable Photonic Crystal Array. Angewandte Chemie, 2015, 127, 12603-12607.	2.0	16
175	Response of the tooth-periodontal ligament-bone complex to load: A microCT study of the minipig molar. Journal of Structural Biology, 2019, 205, 155-162.	2.8	16
176	A 3D study of the relationship between leaf vein structure and mechanical function. Acta Biomaterialia, 2019, 88, 111-119.	8.3	15
177	High resolution 3D structures ofÂmineralized tissues in health andÂdisease. Nature Reviews Endocrinology, 2021, 17, 307-316.	9.6	15
178	Fluorescent Silica Nanoparticles to Label Metastatic Tumor Cells in Mineralized Bone Microenvironments. Small, 2021, 17, e2001432.	10.0	14
179	Koi Fishâ€Scale Iridophore Cells Orient Guanine Crystals to Maximize Light Reflection. ChemPlusChem, 2017, 82, 914-923.	2.8	14
180	A 10,400-year-old sunken lime kiln from the Early Pre-Pottery Neolithic B at the Nesher-Ramla quarry (el-Khirbe), Israel. Journal of Archaeological Science: Reports, 2017, 14, 353-364.	0.5	13

#	Article	IF	CITATIONS
181	Open questions on the 3D structures of collagen containing vertebrate mineralized tissues: A perspective. Journal of Structural Biology, 2018, 201, 187-198.	2.8	13
182	Determining the elastic modulus of mouse cortical bone using electronic speckle pattern interferometry (ESPI) and micro computed tomography: A new approach for characterizing small-bone material properties. Bone, 2009, 45, 84-90.	2.9	12
183	Structure-function relations of primate lower incisors: a study of the deformation of Macaca mulatta dentition using electronic speckle pattern interferometry (ESPI). Journal of Anatomy, 2011, 218, 87-95.	1.5	12
184	Structure and Morphology of Light-Reflecting Synthetic and Biogenic Polymorphs of Isoxanthopterin: A Comparison. Chemistry of Materials, 2019, 31, 4479-4489.	6.7	12
185	An unusual disordered alveolar bone material in the upper furcation region of minipig mandibles: A 3D hierarchical structural study. Journal of Structural Biology, 2019, 206, 128-137.	2.8	12
186	The PteropodCreseis aciculaForms Its Shell through a Disordered Nascent Aragonite Phase. Crystal Growth and Design, 2019, 19, 2564-2573.	3.0	12
187	Controlled Occlusion of Proteins: A Tool for Modulating the Properties of Skeletal Elements. Molecular Crystals and Liquid Crystals, 1994, 248, 185-198.	0.3	11
188	The Chronology of the Late Bronze (LB)-Iron Age (IA) Transition in the Southern Levant: A Response to Finkelstein's Critique. Radiocarbon, 2019, 61, 1-11.	1.8	11
189	Unique three-dimensional structure of a fish pharyngeal jaw subjected to unusually high mechanical loads. Journal of Structural Biology, 2020, 211, 107530.	2.8	10
190	A unique methionine-rich protein–aragonite crystal complex: Structure and mechanical functions of the Pinctada fucata bivalve hinge ligament. Acta Biomaterialia, 2019, 100, 1-9.	8.3	9
191	Characterization of the growth plate-bone interphase region using cryo-FIB SEM 3D volume imaging. Journal of Structural Biology, 2021, 213, 107781.	2.8	9
192	Heating of flint artifacts from the site of Boker Tachtit (Israel) was not detected using FTIR peak broadening. Journal of Archaeological Science: Reports, 2017, 12, 173-182.	0.5	8
193	Reconstructing Ancient Israel: Integrating Macro- and Micro-archaeology. Hebrew Bible and Ancient Israel, 2012, 1, 133.	0.1	6
194	The gizzard plates in the Cephalaspidean gastropod Philine quadripartita: Analysis of structure and function. Quaternary International, 2015, 390, 4-14.	1.5	6
195	Archaeological Ceramic Diagenesis: Clay Mineral Recrystallization in Sherds from a Late Byzantine Kiln, Israel. Minerals (Basel, Switzerland), 2020, 10, 408.	2.0	6
196	Microstructural heterogeneity of the collagenous network in the loaded and unloaded periodontal ligament and its biomechanical implications. Journal of Structural Biology, 2021, 213, 107772.	2.8	6
197	The shell microstructure of the pteropod Creseis acicula is composed of nested arrays of S-shaped aragonite fibers: A unique biological material. MRS Bulletin, 2022, 47, 18-28.	3.5	6
198	Micro-printing with crystal inks. Nature, 1999, 398, 461-462.	27.8	5

#	Article	IF	CITATIONS
199	Identifying a Roman Casting Pit at Tel Dor, Israel: Integrating Field and Laboratory Research. Journal of Field Archaeology, 2009, 34, 135-151.	1.3	5
200	High temperature pyrotechnology: A macro- and microarchaeology study of a late Byzantine-beginning of Early Islamic period (7th century CE) pottery kiln from Tel Qatra/Gedera, Israel. Journal of Archaeological Science: Reports, 2020, 31, 102263.	0.5	5
201	Calcium Sulfate Hemihydrate (Bassanite) Crystals in the Wood of the Tamarix Tree. Minerals (Basel,) Tj ETQq1 1 C	0.784314 r 2.0	ggT /Overic
202	Control Over Aragonite Crystal Nucleation and Growth: An In Vitro Study of Biomineralization. Chemistry - A European Journal, 1998, 4, 389-396.	3.3	5
203	Calcium Ion and Mineral Pathways in Biomineralization: A Perspective. , 2018, , 97-103.		4
204	Structural organization of xanthine crystals in the median ocellus of a member of the ancestral insect group Archaeognatha. Journal of Structural Biology, 2022, 214, 107834.	2.8	4
205	Microflint in archaeological sediments from Boker Tachtit, Israel: A new method for quantifying concentrations of small flint fragments. Journal of Archaeological Science, 2018, 91, 52-64.	2.4	2
206	Control Over Aragonite Crystal Nucleation and Growth: An In Vitro Study of Biomineralization. , 1998, 4, 389.		2
207	Characterization and possible function of an enigmatic reflector in the eye of the shrimp Litopenaeus vannamei. Faraday Discussions, 2020, 223, 278-294.	3.2	2
208	Microarchaeology at Tell eṣ-Ṣâfi/Gath, Area A. Near Eastern Archaeology, 2018, 81, 24-27.	0.2	0
209	A powder preparation kit from the Middle Bronze Age at Megiddo, Israel: Tools and raw materials. Journal of Archaeological Science: Reports, 2018, 21, 667-678.	0.5	0
210	Chalcolithic groundwater mining in the southern Levant: open, vertical shafts in the Late Chalcolithic central coastal plain settlement landscape of Israel. Levant, 2019, 51, 236-270.	0.9	0
211	Natural Photonic Structures from Birefringent Core-Shell Nanoparticles. Optics and Photonics News, 2020, 31, 51.	0.5	0